

# New Dual-Functional and Reusable Bimetallic $Y_2ZnO_4$ Nanocatalyst for Organic Transformation under Microwave/Green Conditions

Mithun Kumar Ghosh, Kavita Jain, Siddique Khan, Kalpataru Das,\* and Tanmay Kumar Ghorai\*



Cite This: *ACS Omega* 2020, 5, 4973–4981



Read Online

ACCESS |



Metrics & More

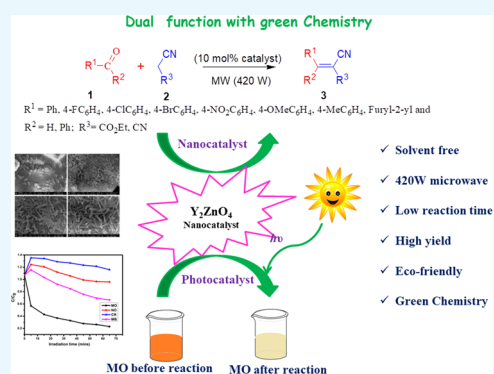


Article Recommendations



Supporting Information

**ABSTRACT:** A novel bimetallic and reusable  $Y_2ZnO_4$  nanocatalyst was synthesized by a simple coprecipitation method. The prepared nanocatalyst exhibited dual catalytic activity and was characterized using X-ray diffraction (XRD), Fourier transform infrared spectroscopy (FT-IR), energy-dispersive X-ray spectroscopy (EDX), and scanning electron microscopy (SEM). The average crystallite and grain sizes were found to be  $17 \pm 1$  and  $10 \pm 2$  nm, respectively. On the one hand, the catalytic activity of the nanocatalyst was studied for the Knoevenagel condensation reaction of aromatic aldehydes with active methylene compounds, such as ethyl cyanoacetate and malononitrile, under microwave irradiation and solvent-free conditions. On the other hand, the nanoparticles also showed faster photocatalytic activity against methyl orange (MO) compared to other dyes. The nanocatalyst was easily recoverable by a simple filtration method and was recycled without any significant loss of catalytic activity. The advantages of this nanocatalyst were a simple workup procedure, high reaction yields, solvent-free conditions, reusability, and a short reaction time under green reaction conditions.



## INTRODUCTION

In recent years, nanocatalysts have increasingly attracted attention in the development of chemical reactions under green reaction conditions. Some of the progressive areas of green chemistry are the solvent-free and microwave conditions used for various types of organic reactions with nanocatalysts as heterogeneous catalysts. Metal oxides and, particularly, bimetallic oxide nanoparticles have several applications including as catalysts,<sup>1</sup> photocatalysts,<sup>2</sup> antimicrobial agents,<sup>3</sup> materials with magnetic properties,<sup>4</sup> and CT-DNA binding agents.<sup>5</sup> The most attractive feature of nanoparticles lies in the field of green chemistry as they serve as green catalysts in organic reactions and have advantages such as easy separation from the reaction mixture by simple filtration, reusability, recyclability, and environmental friendliness.<sup>6,7</sup>

Many conventional organic reactions need high temperatures and long reaction times. However, microwave (MW) irradiation techniques accelerated the rate of organic reactions dramatically, and the reactions were accomplished within a shorter reaction time. Owing to these attractive features, microwave-assisted functional group transformations and chemical synthesis gained tremendous interest in the field of green and sustainable chemistry. On the other hand, avoiding toxic and volatile organic solvents is the most acceptable practice in green chemical synthesis, and accordingly, development of solvent-free reaction conditions is a highly desirable process in terms of cost and environmental benefits.<sup>8–21</sup>

The Knoevenagel condensation is one of the most important reactions in organic synthesis involving C–C bond-forming

reactions. The applications of the Knoevenagel reaction are enormous, including the synthesis of fine chemicals, anticoagulants, antibacterial agents, fungicides, pesticides, etc.<sup>22–25</sup> The Knoevenagel condensation is facilitated mainly in the presence of bases, a catalyst such as piperidine, pyridine, sodium ethoxide, and ammonia, and other organocatalysts.<sup>26</sup> Some metal oxides also serve as catalysts in the Knoevenagel condensation, such as  $ZrO_2$ ,<sup>27</sup>  $TiO_2$ ,<sup>28,29</sup>  $Fe_3O_4$ ,<sup>30</sup>  $NiO$ ,<sup>31,32</sup> and  $CuO$ .<sup>33,34</sup> However, most of the reported works have one or several drawbacks, such as the use of toxic organic solvents, long reaction times, and nonseparable, nonrecyclable, expensive, and toxic catalyst systems. Thus, it was desirable to develop an efficient catalytic approach for the Knoevenagel condensation under green reaction conditions. In continuation of our research work toward the development of efficient multifunctional and recyclable catalysts, we wish to report an ecofriendly and green protocol for the Knoevenagel condensation using the bimetallic oxide,  $Y_2ZnO_4$ , as a nontoxic nanocatalyst under microwave and solvent-free reaction conditions.

**Received:** November 13, 2019

**Accepted:** February 19, 2020

**Published:** March 5, 2020



The efficiency of the nanocatalyst was further demonstrated by the photocatalytic degradation of a dye, methyl orange (MO), under green conditions. Pollutant dyes come from different sources, such as textile, paper, cosmetic, and plastic industries, and so on.<sup>35–37</sup> Non-biodegradable dyes can cause a variety of diseases, such as skin rashes, allergies, and liver and kidney damage.<sup>38,39</sup> Therefore, non-biodegradable dyes must be removed from drinking water.

In this work, we synthesized the  $Y_2ZnO_4$  nanocatalyst using a simple coprecipitation method, and it was characterized by X-ray diffraction (XRD), Fourier transform infrared spectroscopy (FT-IR), energy-dispersive X-ray spectroscopy (EDX), and scanning electron microscopy (SEM). The nanoparticles were used as a photocatalyst against methyl orange (MO) and as a catalyst to perform the Knoevenagel reaction between aromatic aldehydes with active methylene compounds, such as ethyl cyanoacetate and malononitrile, under solvent-free, microwave (MW) conditions.

**Green Context.** Bimetallic oxide  $Y_2ZnO_4$  was used as a nontoxic and recyclable nanocatalyst in both Knoevenagel condensation and photocatalytic dye degradation under green conditions. The use of microwave (MW) radiation dramatically enhanced the reaction rate, and the Knoevenagel reaction was accomplished in a shorter reaction time with high conversion and selectivity under solvent-free conditions. The described methodology has several advantages over conventional methods because in this green approach, the nanocatalyst is easily separable and recoverable from the product. This approach avoided the use of toxic organic solvents, and there was no formation of byproducts as waste in the Knoevenagel condensation. Moreover, degradation of the pollutant dye, methyl orange, was carried out using the nanoparticles as the catalyst by following the concept of green chemistry in the presence of sunlight.

## RESULTS AND DISCUSSION

**XRD Analysis.** The XRD technique was used to determine and confirm the crystal structure of  $Y_2ZnO_4$ . The intense diffraction peaks observed at 34.63, 36.48, 37.90, 45.88, 58.30, and 63.25° were indexed to the (100), (002), (101), (102), (110), and (103) planes, respectively,<sup>3</sup> as shown in Figure 1. The crystallite size of  $Y_2ZnO_4$  was  $17 \pm 1$  nm, measured using the Scherrer method.

**SEM and EDX Analysis.** Scanning electron microscopy (SEM) studies were performed on  $Y_2ZnO_4$  to gain information about the grain size. Figure 2 represents the SEM images of

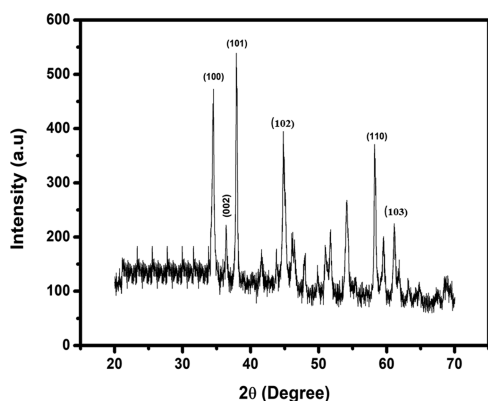


Figure 1. XRD pattern of  $Y_2ZnO_4$ .

$Y_2ZnO_4$  at different resolutions. The SEM images show that the nanomaterials are rod-shaped, paddy-seed-like particles and that they are arranged in a well-ordered manner, with the average grain size of the nanoparticles being  $10 \pm 2$  nm. The elemental description of the sample was obtained from energy-dispersive X-ray (EDX) analysis and the % elemental composition is shown in Figure S1 and Table S1. The peaks located at 1 and 2 keV are directly related to the characteristics of zinc and yttrium.

**FT-IR Analysis.** The FT-IR spectrum of  $Y_2ZnO_4$  is presented in Figure S2. The band observed at about  $3436 \text{ cm}^{-1}$  was characteristic of the H–O bending mode of the hydroxyl groups present on the surface due to moisture. The peak appearing at about  $675 \text{ cm}^{-1}$  was due to the bending vibration of the Zn–O bond.<sup>25b</sup>

**Knoevenagel Condensation Using  $Y_2ZnO_4$  as the Nanocatalyst.** The optimization of the Knoevenagel condensation was performed using commercially available benzaldehyde **1a** and ethyl cyanoacetate **2a** in the presence of the synthesized nanocatalyst,  $Y_2ZnO_4$ .

Initially, we carried out the Knoevenagel reaction under solvent-free conditions at room temperature using 10 mol %  $Y_2ZnO_4$  nanocatalyst and detected the formation of the Knoevenagel condensation product, **3a**, as observed from the  $^1\text{H}$  NMR spectrum of the crude reaction mixture. However, at room temperature, the reaction was not completed after 5 h and the yield of the reaction was found to be poor (Table 1, entry 1). With this encouraging result, we carried out the optimization of the Knoevenagel condensation using  $Y_2ZnO_4$  as the nanocatalyst and screened various reaction conditions, such as room temperature, catalyst loading, solvent-free conditions, effect of solvents, and conventional heating, followed by the effect of microwave (MW) radiation. The optimization results are summarized in Tables 1 and 2. When the reaction was performed at 70 °C, the yield of the condensation product **3a** was improved to 56% using the same catalyst loading under solvent-free conditions (Table 1, entry 2). The Knoevenagel product, **3a**, was confirmed by  $^1\text{H}$  NMR spectroscopic data and comparison with literature data.<sup>40–45</sup> A decrease in reaction yield was noted when we performed the reaction using a lower catalyst loading (Table 1, entry 3). Next, we studied the effect of solvent on the catalytic reaction in the presence of 10 mol % nanocatalyst ( $Y_2ZnO_4$ ). It was observed that the yield of product **3a** was found to be better in ethanol and methanol (Table 1, entries 7 and 11) than in other solvents under heating conditions. However, conventional heating was found to be very slow and the reaction was not completed even after 5 h. To improve the efficiency of the Knoevenagel reaction and yield of **3a**, we exploited the microwave (MW) effect on the catalytic reaction using the nanocatalyst ( $Y_2ZnO_4$ ). In recent years, microwave-assisted synthesis has become highly attractive and useful for the development of green and sustainable processes.<sup>8</sup> Subsequently, we further optimized the reaction under microwave irradiation, employing the same nanocatalyst (10 mol %  $Y_2ZnO_4$ ) under solvent-free conditions. The optimization of the Knoevenagel reaction under microwave irradiation is shown in Table 2. When the reaction mixture was irradiated at 140 W, within a short period of time, the formation of **3a** was observed and the NMR yield was found to be 70% (Table 2, entry 1).

A variation in reaction yield was observed when the microwave irradiation power was varied. The reaction was

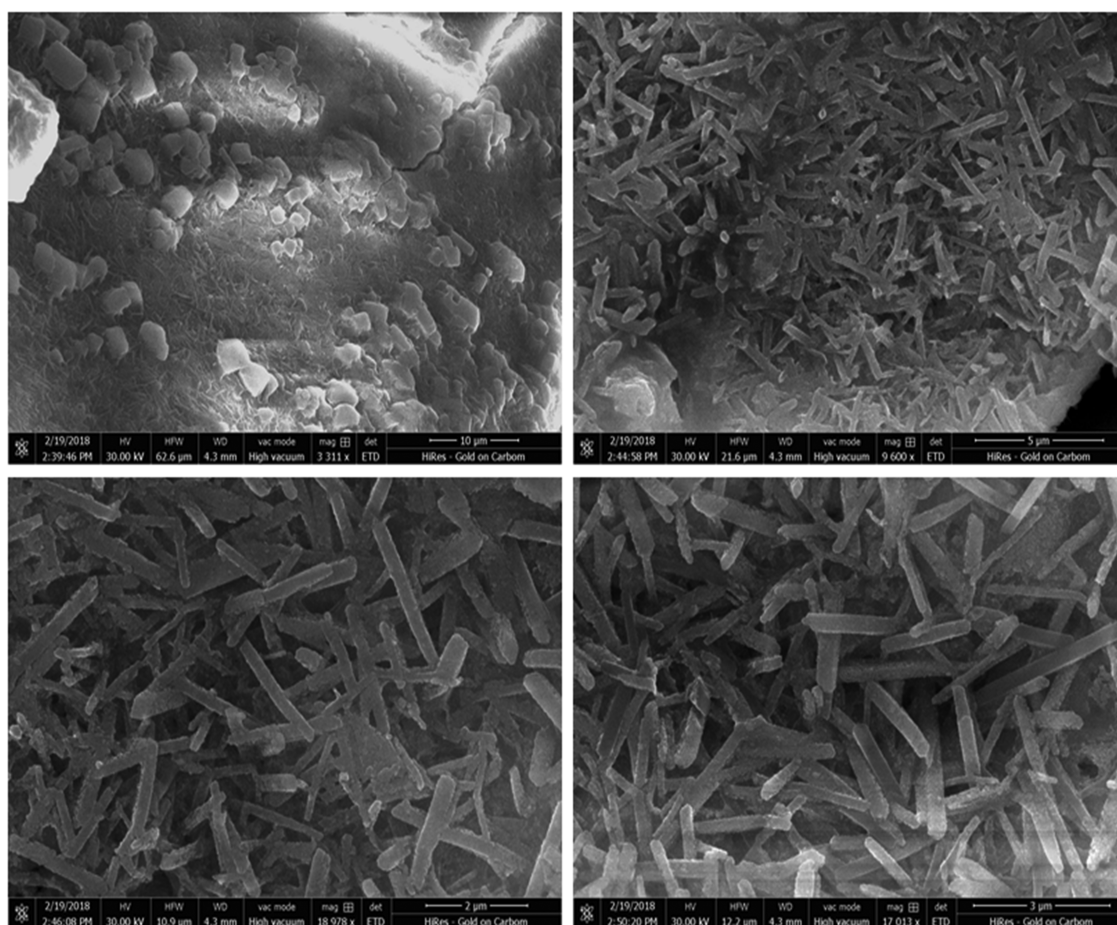
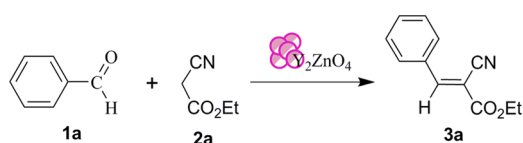


Figure 2. SEM image of  $Y_2ZnO_4$  at different resolutions.

Table 1. Optimization of the Knoevenagel Condensation Using Nanocatalyst  $Y_2ZnO_4$ <sup>a</sup>

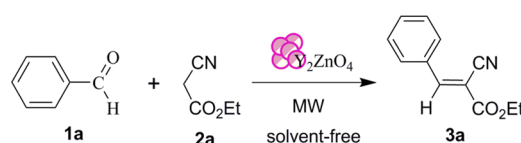


entry	solvent	nanocatalyst (mol %)	time (h)	condition	yield (%) <sup>b</sup>
1	no solvent	$Y_2ZnO_4$ (10%)	5	RT	41
2	no solvent	$Y_2ZnO_4$ (10%)	5	70 °C	56
3	no solvent	$Y_2ZnO_4$ (05%)	5	70 °C	48
4	$H_2O$	$Y_2ZnO_4$ (10%)	5	RT	nd <sup>c</sup>
5	$H_2O$	$Y_2ZnO_4$ (10%)	5	70 °C	nd <sup>c</sup>
6	$CH_3OH$	$Y_2ZnO_4$ (10%)	5	RT	nd <sup>c</sup>
7	$CH_3OH$	$Y_2ZnO_4$ (10%)	5	70 °C	42
8	$CH_3CN$	$Y_2ZnO_4$ (10%)	5	RT	nd <sup>c</sup>
9	$CH_3CN$	$Y_2ZnO_4$ (10%)	5	70 °C	nd <sup>c</sup>
10	$C_2H_5OH$	$Y_2ZnO_4$ (10%)	5	RT	nd <sup>c</sup>
11	$C_2H_5OH$	$Y_2ZnO_4$ (10%)	5	70 °C	62

<sup>a</sup>Reaction conditions: Unless otherwise mentioned, the reaction was carried out with benzaldehyde **1a** (0.530 mmol, 56.2 mg), ethyl cyanoacetate **2** (0.442 mmol, 50 mg), and nanocatalyst  $Y_2ZnO_4$  (10 mol %, 0.044 mmol, 13.6 mg) at room temperature (RT). <sup>b</sup>Yield of **3a** was determined by <sup>1</sup>H NMR analysis. <sup>c</sup>Not determined (nd).

found to be completed within 15 min when the microwave irradiation power was increased to 420 W, and the yield was

Table 2. Optimization of the Knoevenagel Condensation under Microwave (MW) Conditions<sup>a</sup>



entry	nanocatalyst (mol %)	time (min)	condition <sup>a</sup>	yield (%) <sup>b</sup>
1	$Y_2ZnO_4$ (10%)	15	MW 140 W	70
2	$Y_2ZnO_4$ (10%)	15	MW 280 W	79
3	$Y_2ZnO_4$ (10%)	15	MW 420 W	92
4	$Y_2ZnO_4$ (10%)	10	MW 420 W	78
5	$Y_2ZnO_4$ (20%)	10	MW 420 W	86

<sup>a</sup>Reaction conditions: Unless otherwise mentioned, the reaction was carried out with benzaldehyde **1a** (0.530 mmol, 56.2 mg), ethyl cyanoacetate **2** (0.442 mmol, 50 mg), and nanocatalyst  $Y_2ZnO_4$  (10 mol %, 0.044 mmol, 13.6 mg) under microwave (MW) and solvent-free conditions. <sup>b</sup>Yield of **3a** was determined by <sup>1</sup>H NMR analysis.

increased to 92% (Table 2, entry 3). The effect of microwave irradiation power on the yield of **3a** is depicted in Figure 3. Under the same reaction conditions, the yield of **3a** was decreased when the reaction time was reduced to 10 min (Table 2, entry 4). Similarly, a reduced yield of **3a** was observed when the catalyst loading was increased to 20 mol % (Table 2, entry 5). Under microwave irradiation, we achieved the best reaction condition at 420 W in the presence of 10 mol % nanocatalyst under solvent-free conditions (Table 2, entry



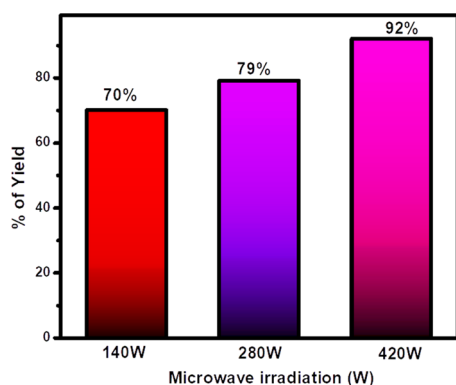


**Figure 3.** Effect of microwave irradiation power on the yield of product 3a.

3). The effect of microwave irradiation power on the yield of 3a was studied, and we observed that the yield of 3a was increased by increasing the microwave power, as depicted in Figure 3.

After the optimization of the reaction and determination of the best reaction condition using  $Y_2ZnO_4$  as the nanocatalyst under microwave and solvent-free conditions, as shown in Table 2, entry 3, we next evaluated the scope and efficiency of the Knoevenagel condensation. Under the optimized condition, a range of aromatic carbonyl compounds **1** reacted smoothly with ethyl cyanoacetate **2a** ( $R^3 = CO_2Et$ ) and afforded the corresponding Knoevenagel condensation products (**3a–l**) with up to 92% yield within a short period of time (Table 3).

No significant difference in the rate of reaction was found between various aromatic aldehydes containing electron-withdrawing and electron-donating groups under our reaction conditions. However, an aromatic ketone, such as benzophenone, reacted with a comparatively slower reaction rate to afford the corresponding Knoevenagel product, **3h** (Table 3, entry 8). Under microwave conditions, heteroaromatic aldehyde furfural also reacted efficiently with ethyl cyanoacetate and afforded product **3i** via the Knoevenagel condensation, as shown in Table 3, entry 9. Next, the substrate scope of the reaction was further evaluated using malononitrile as the active methylene compound. Under the optimized condition, aromatic carbonyl compounds reacted smoothly with malononitrile and afforded the corresponding Knoevenagel condensation products (**3j–l**) within a short period of time, as shown in Table 3 (entries 10–12). The structure of all products (**3a–l**) was determined by  $^1H$  NMR data and comparison with literature data.<sup>40–44</sup> Compared to the reported methods, our method under microwave conditions is environmentally friendly and has several advantages including a short reaction time and solvent-free conditions with excellent conversion and yields. Moreover, the reaction does not require any additive or activators and the nanocatalyst used in the reaction is easily recoverable and recyclable.

**Reusability of Nanocatalyst  $Y_2ZnO_4$ .** After completion of the first run, diethyl ether was added to the reaction mixture and nanocatalyst  $Y_2ZnO_4$  was recovered by simple filtration. The recovered catalyst was washed repeatedly with diethyl ether and dried at 100 °C in a hot air oven for reuse. The recyclability of the catalyst was studied for the Knoevenagel condensation under the optimized reaction condition. The catalyst recovered in the first run was reused in two more

subsequent runs without any appreciable loss of catalytic activity (Figure 4).

Before and after the catalytic reaction, we studied the morphology of the  $Y_2ZnO_4$  nanoparticle using SEM. After the reaction, the morphology was slightly changed, as shown in Figure 5; however, no loss of appreciable catalytic activity was observed in the subsequent runs. This is due to the high stability of nanocatalyst  $Y_2ZnO_4$  under our reaction conditions.

#### Mechanistic Pathway of the Knoevenagel Reaction.

According to the literature<sup>6</sup> and based on the above experimental facts, a possible reaction mechanism of the Knoevenagel reaction catalyzed by nanocatalyst  $Y_2ZnO_4$  under microwave (MW) conditions is proposed in Scheme 1. In the first step, benzaldehyde **1a** is activated by forming a complex between the carbonyl oxygen and the nanocatalyst. After that, the activated aldehyde complex **4** is attacked by the active methylene compound, ethyl cyanoacetate, generating an intermediate **5**. Intermediate **5** is then protonated and activated by the nanocatalyst through coordination with a hydroxyl group, leading to the formation of complex **6**. The elimination of water from intermediate **6** subsequently affords the corresponding product **3a**. The high catalytic activity observed in this reaction is probably due to the large surface area of the nanoparticles.

**Photocatalytic Activity.** The photocatalytic activity of nanocatalyst  $Y_2ZnO_4$  against different types of organic dyes, such as methyl orange (MO), methylene blue (MB), naphthol orange (NO), and congo red (CR), was studied in the presence of sunlight. The efficiency of a catalyst for the degradation of a dye is defined in terms of  $C/C_0$ , where  $C$  and  $C_0$  represent the final and initial concentrations of the dye (Figure 6a). Among all dyes, MO was degraded faster compared with the other dyes and completely decolorized within 65 min in the presence of nanoparticles and sunlight (Figure 6a), whereas the other dyes, MB, NO, and CR, were not degraded. This is due to the lower energy band gap (2.7 eV) of nanocatalyst  $Y_2ZnO_4$  calculated from optical spectra. According to Beer–Lambert’s law, the concentration of MO is linearly proportional to the intensity of the absorption peak of MO at 463 nm, and the efficiency of the nanocatalyst for degradation of MO can be calculated using the following eq 1

$$\text{efficiency (\%)} = \left(1 - \frac{A_t}{A_0}\right) \times 100 \quad (1)$$

where  $A_t$  and  $A_0$  are the absorbance of the dye at time  $t$  and at the initial time, respectively. The degradation efficiency of nanocatalyst  $Y_2ZnO_4$  is about 78.5% against MO and the corresponding rate constant ( $k$ ) is about  $3.939 \times 10^{-4} s^{-1}$ . The absorption spectra of methyl orange at a constant time interval were investigated and are shown in Figure 6b. The optical band gap was calculated according to our previous publication.<sup>46</sup> The optical band gap value was 2.7 eV, which was supported by a literature review.<sup>3</sup> The proposed mechanism pathway for the degradation of MO in the presence of the nanocatalyst and sunlight is shown in Figure 7.

## CONCLUSIONS

In the above experiment, we synthesized a nanocatalyst  $Y_2ZnO_4$  by a simple coprecipitation method. Nanocatalyst  $Y_2ZnO_4$  has excellent dual catalytic activity; one of them is in the Knoevenagel reaction under microwave and solvent-free conditions to afford a range of substituted alkenes and the



Table 3. Knoevenagel Condensation under the Optimized Condition<sup>a</sup>

R<sup>1</sup> = Ph, 4-FC<sub>6</sub>H<sub>4</sub>, 4-ClC<sub>6</sub>H<sub>4</sub>, 4-BrC<sub>6</sub>H<sub>4</sub>, 4-NO<sub>2</sub>C<sub>6</sub>H<sub>4</sub>, 4-OMeC<sub>6</sub>H<sub>4</sub>, 4-MeC<sub>6</sub>H<sub>4</sub>, Furyl-2-yl and  
R<sup>2</sup> = H, Ph; R<sup>3</sup> = CO<sub>2</sub>Et, CN

Entry	R <sup>1</sup> , R <sup>2</sup>	Product (3)	Time(min)	Literature yield (%) <sup>b</sup>	Yield(%) <sup>c</sup>
1	Ph, H		15	86 <sup>40</sup>	92
2	4-FC <sub>6</sub> H <sub>5</sub> , H		10	94 <sup>41</sup>	81
3	4-ClC <sub>6</sub> H <sub>5</sub> , H		12	70 <sup>40</sup>	79
4	4-BrC <sub>6</sub> H <sub>5</sub> , H		12	70 <sup>40</sup>	83
5	4-NO <sub>2</sub> C <sub>6</sub> H <sub>5</sub> , H		10	85 <sup>42</sup>	88
6	4-OMeC <sub>6</sub> H <sub>5</sub> , H		12	59 <sup>40</sup>	90
7	4-MeC <sub>6</sub> H <sub>5</sub> , H		25	73 <sup>40</sup>	86
8	Ph, Ph		30	64 <sup>43</sup>	85
9	Furyl, H		15	85 <sup>44</sup>	84
10	Ph, H		15	80 <sup>42</sup>	84
11	4-MeC <sub>6</sub> H <sub>5</sub> , H		15	79 <sup>42</sup>	84
12	4-NO <sub>2</sub> C <sub>6</sub> H <sub>5</sub> , H		10	81 <sup>42</sup>	62

<sup>a</sup>Reaction conditions: Unless otherwise mentioned, the reaction was carried out with aromatic aldehyde **1** (0.530 mmol, 56.2 mg), ethyl cyanoacetate **2** (0.442 mmol, 50 mg), and nanocatalyst Y<sub>2</sub>ZnO<sub>4</sub> (10 mol %, 0.044 mmol, 13.6 mg) under MW (420 W) and solvent-free conditions.  
<sup>b</sup>Literature yield. <sup>c</sup>Yield of **3** was determined by <sup>1</sup>H NMR analysis.

other one is as a photocatalyst for the degradation of MO. The reported method for the Knoevenagel reaction is commercially

highly interesting because of several advantages, including mild reaction conditions, a green process, easy recovery and

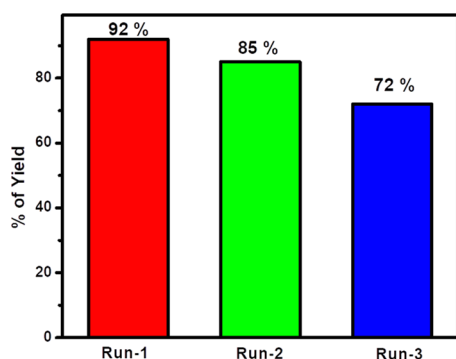


**Figure 4.** Recycling of nanocatalyst  $Y_2ZnO_4$  in the Knoevenagel condensation.

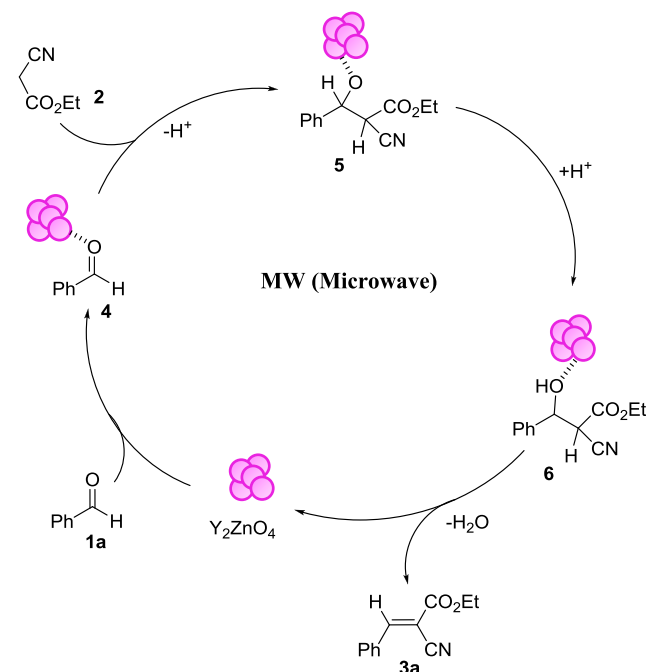
reusability of the catalyst, excellent yields, short reaction times, and an ecofriendly approach. The photocatalytic activity of  $Y_2ZnO_4$  helps degrade the dye molecules and reduces harmful pollutants from the environment. Antimicrobial activity and other applications of  $Y_2ZnO_4$  will be studied in further work.

## EXPERIMENTAL SECTION

**Materials and Apparatus.** All required chemicals were purchased from Sigma-Aldrich and Merck. All chemicals were used without purification.

The Knoevenagel reaction was performed under microwave conditions. The microwave synthesis was carried out using a domestic microwave oven (2450 MHz, 1050 W) in a screw cap glass tube. The crystal structure of  $Y_2ZnO_4$  was studied by X-ray diffraction (XRD) at room temperature using a D8 Advance Bruker, equipped with  $Cu K\alpha$  (1.54060 Å) as the incident radiation. The Scherrer equation was used for the calculation of crystal size. The Scherrer equation is  $D = K\lambda / \beta \cos \theta$ ,  $K = 0.9$ ,  $D =$  crystal size (Å),  $\lambda =$  wavelength of  $Cu K\alpha$  radiation, and  $\beta =$  corrected half-width of the diffraction peak. The IR spectra were recorded on a Shimadzu FTIR-8400S spectrometer at room temperature. The fine structure of the prepared samples was analyzed by scanning electron microscopy (SEM) (Carl Zeiss Germany, Model Supra-40). Energy-dispersion X-ray spectroscopy (EDX) of nanoparticles was performed on a Sigma ZEISS, Oxford Instruments field emission microscope. The  $^1H$  NMR spectra were recorded on a JEOL-400 MHz spectrometer using chloroform- $D$  ( $CDCl_3$ ) as the solvent and tetramethylsilane (TMS) as an internal standard. The chemical shifts are reported in ppm relative to

## Scheme 1. Proposed Mechanism for the Knoevenagel Condensation Catalyzed by $Y_2ZnO_4$



TMS at  $\delta$  0.00 ppm.  $^1H$  NMR splitting patterns are designated as singlet (s), broad singlet (br. s), doublet (d), triplet (t), quartet (q), or multiplet (m).

**Synthesis of Nanocatalyst  $Y_2ZnO_4$ .** The total synthesis of the nanocatalyst was carried out by a coprecipitation method.  $Y(NO_3)_3 \cdot 6H_2O$  was dissolved in a minimum volume of distilled water (set-1).  $ZnO$  was also dissolved in minimum amounts of water and dil. HCl (set-2). Now, 20 mL of  $C_2H_5OH$  was added into set-1, and it was poured into set-2 with constant stirring with a magnetic stirrer for 30 min. A clear solution was obtained; then,  $NH_4OH$  was added dropwise to maintain the pH (8–9), and a white gelatinous precipitate was produced, which was filtered. The precipitate washed with water and dried at about  $600^\circ C$  for 2 h. The yield was 81.7% with respect to the starting materials.

**General Procedure for the Knoevenagel Condensation Using  $Y_2ZnO_4$  as the Nanocatalyst.** A mixture of benzaldehyde **1a** (0.530 mmol, 56.2 mg), ethyl cyanoacetate **2** (0.442 mmol, 50 mg), and  $Y_2ZnO_4$  nanopowder (10 mol %,

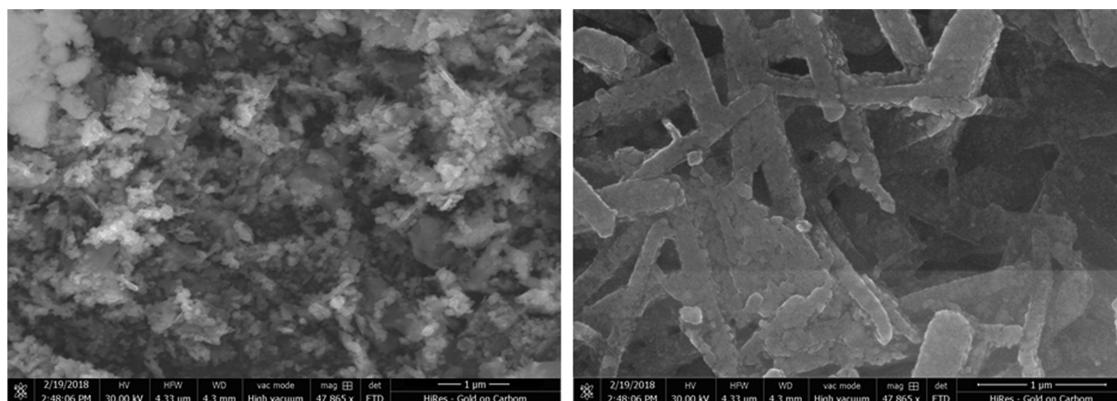


**Figure 5.** SEM image of nanocatalyst  $Y_2ZnO_4$  after the reaction.

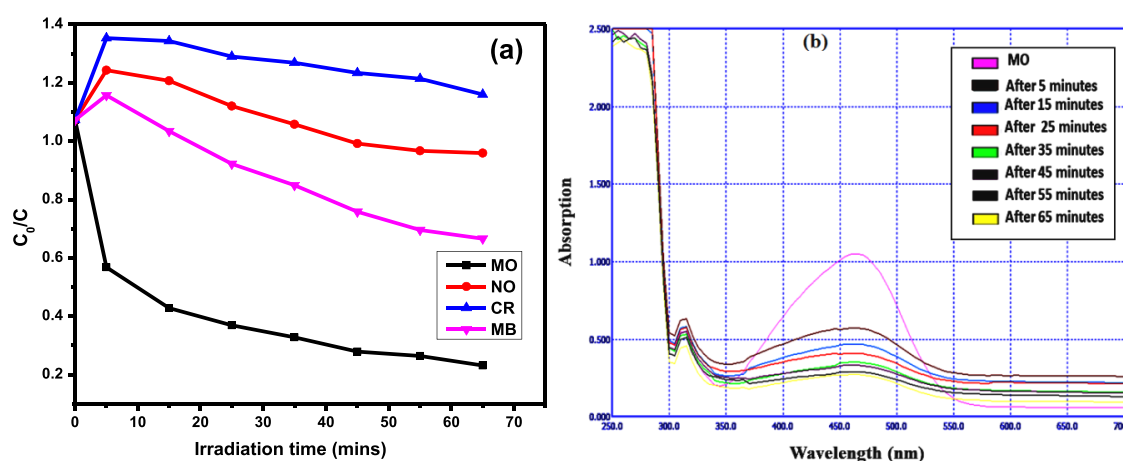


**Figure 6.** Photodegradation of different dyes by the nanocatalyst as a normalized change in the concentration as a function of irradiation time (a) and absorption spectra of the MO solution in the presence of the nanocatalyst under sunlight (b).

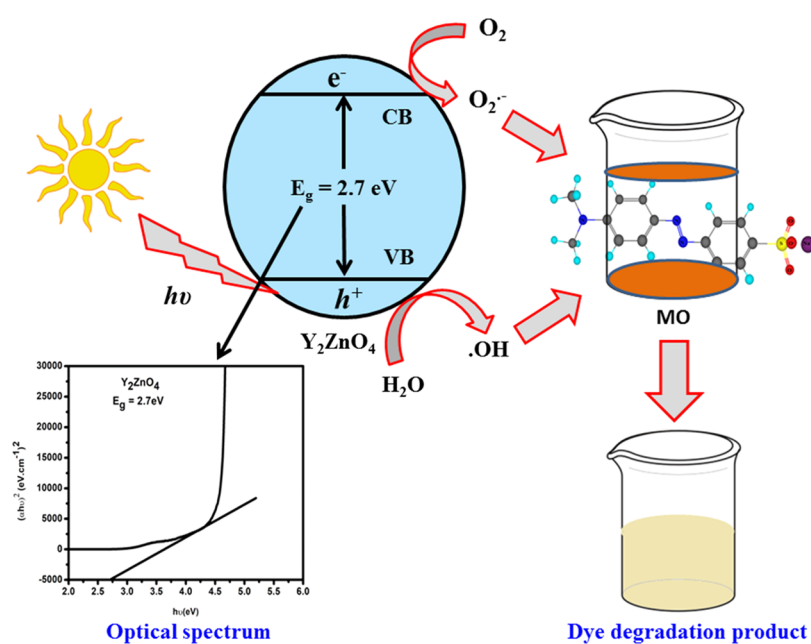


**Figure 7.** Proposed mechanism for MO degradation in the presence of the nanocatalyst and sunlight.

0.044 mmol, 13.6 mg) was taken in a screw cap glass tube and subjected to microwave irradiation at 420 W. The reaction was monitored by thin layer chromatography (TLC) using 10% ethyl acetate in *n*-hexane. After 15 min, the reaction was found to be completed. Then, the glass tube was cooled and diluted with diethyl ether (5 mL). The catalyst was separated by filtration. The catalyst was washed thoroughly with diethyl ether (5 mL) and dried in a hot air oven for reuse. The combined ether was evaporated to dryness to obtain the crude product. The yield of the product was determined from the  $^1H$  NMR analysis of the crude reaction mixture. The yield of product 3a was found to be 92% (Table 3, entry 1). All products shown in Table 3 were synthesized according to the above procedure and were confirmed by  $^1H$  NMR spectral data and comparison with literature data (see the Supporting Information).

**Dye Degradation.** Rhodamine B (RB), methyl orange (MO), naphthyl orange (NO), and methylene blue (MB) were separately dissolved in water. Then, 10 mg of the nanocatalyst was soaked in 10 mL of dye solution and kept in sunlight.

Furthermore, we examined the specific photocatalytic activity, and readings from the UV spectrometer were taken regularly.

## ■ ASSOCIATED CONTENT

### Supporting Information

The Supporting Information is available free of charge at <https://pubs.acs.org/doi/10.1021/acsomega.9b03875>.

EDAX data, FT-IR data, and  $^1H$  NMR data (Figures S1–11 and Table S1) (PDF)

## ■ AUTHOR INFORMATION

### Corresponding Authors

Kalpataru Das – Advanced Organic Synthesis Laboratory, Department of Chemistry, Dr. Harisingh Gour Vishwavidyalaya (Central University), Sagar 470003, Madhya Pradesh, India; [orcid.org/0000-0003-4592-8796](https://orcid.org/0000-0003-4592-8796); Email: [kalpatarud@gmail.com](mailto:kalpatarud@gmail.com)

Tanmay Kumar Ghorai – Nanomaterials and Crystal Designing Laboratory, Department of Chemistry, Indira Gandhi



National Tribal University, Amarkantak 484887, Madhya Pradesh, India; [orcid.org/0000-0001-8758-7956](https://orcid.org/0000-0001-8758-7956);  
Email: [tanmay.ghorai@igntu.ac.in](mailto:tanmay.ghorai@igntu.ac.in), [tanmayghorai66@gmail.com](mailto:tanmayghorai66@gmail.com)

## Authors

**Mithun Kumar Ghosh** – Nanomaterials and Crystal Designing Laboratory, Department of Chemistry, Indira Gandhi National Tribal University, Amarkantak 484887, Madhya Pradesh, India

**Kavita Jain** – Advanced Organic Synthesis Laboratory, Department of Chemistry, Dr. Harisingh Gour Vishwavidyalaya (Central University), Sagar 470003, Madhya Pradesh, India

**Siddique Khan** – Advanced Organic Synthesis Laboratory, Department of Chemistry, Dr. Harisingh Gour Vishwavidyalaya (Central University), Sagar 470003, Madhya Pradesh, India

Complete contact information is available at:

<https://pubs.acs.org/10.1021/acsomega.9b03875>

## Author Contributions

All experiments and applications were performed by M.K.G., Dr. K.J., and S.K. under the supervision of Dr. T.K.G. and Dr. K.D. The manuscript was written by M.K.G. and reviewed by Dr. T.K.G. and Dr. K.D.

## Notes

The authors declare no competing financial interest.

## ACKNOWLEDGMENTS

This work was fully supported by Madhya Pradesh Council of Science & Technology, Govt. of India, Madhya Pradesh (File no. A/R&D/2/Phy&Engg./2017-18/271), Science and Engineering Research Board (SERB), Govt. of India (File No. EMR/2017/000234), Indira Gandhi National Tribal University, Amarkantak, Madhya Pradesh, India, Dr. Harisingh Gour Vishwavidyalaya (Central University), Sagar, M.P., India, and Guru Ghasidas Vishwavidyalaya (Central University), Bilaspur, C.G.

## REFERENCES

- (1) Lakshminarayana, B.; Mahendar, L.; Ghosal, P.; Sreedhar, B.; Satyanarayana, G.; Subrahmanyam, C. Fabrication of Pd/CuFe<sub>2</sub>O<sub>4</sub> hybrid nanowires: a heterogeneous catalyst for Heck couplings. *New J. Chem.* **2018**, *42*, 1646–1654.
- (2) Jing, L.; Xu, Y.; Chen, Z.; He, M.; Xie, M.; Liu, J.; Xu, H.; Huang, S.; Li, H. Different morphologies of SnS<sub>2</sub> supported on 2D g-C<sub>3</sub>N<sub>4</sub> for excellent and stable visible light photocatalytic hydrogen generation. *ACS Sustainable Chem. Eng.* **2018**, *6*, 5132–5141.
- (3) Mote, V. D.; Purushotham, Y.; Shinde, R. S.; Salunke, S. D.; Dole, B. N. Structural, optical and antibacterial properties of yttrium doped ZnO nanoparticles. *Cerâmica* **2015**, *61*, 457–461.
- (4) Andersen, H. L.; Saura-Múzquiz, M.; Granados-Miralles, C.; Canévet, E.; Lock, N.; Christensen, M. Crystalline and magnetic structure–property relationship in spinel ferrite nanoparticles. *Nano-scale* **2018**, *10*, 14902–14914.
- (5) Elmes, R. B.; Orange, K. N.; Cloonan, S. M.; Williams, D. C.; Gunnlaugsson, T. Luminescent ruthenium(II) polypyridyl functionalized gold nanoparticles; their DNA binding abilities and application as cellular imaging agents. *J. Am. Chem. Soc.* **2011**, *133*, 15862–15865.
- (6) Ghomi, J. S.; Akbarzadeh, Z. Ultrasonic accelerated Knoevenagel condensation by magnetically recoverable MgFe<sub>2</sub>O<sub>4</sub> nanocatalyst: A rapid and green synthesis of coumarins under solvent-free conditions. *Ultrason. Sonochem.* **2018**, *40*, 78–83.
- (7) Lim, C. W.; Lee, I. S. Magnetically recyclable nanocatalyst systems for the organic reactions. *Nano Today* **2010**, *5*, 412–434.

- (8) (a) Varma, R. Solvent-free organic syntheses. using supported reagents and microwave irradiation. *Green Chem.* **1999**, *1*, 43–55. (b) Peng, Y.; Song, G. Combined microwave and ultrasound accelerated Knoevenagel–Doebner reaction in aqueous media: a green route to 3-aryl acrylic acids. *Green Chem.* **2003**, *5*, 704–706.
- (9) Gedye, R.; Smith, F.; Westaway, K.; Ali, H.; Baldisera, L.; Laberge, L.; Rousell, J. The use of microwave ovens for rapid organic synthesis. *Tetrahedron Lett.* **1986**, *27*, 279–282.
- (10) Naeimi, H.; Aghaseyedkarimi, D. Fe<sub>3</sub>O<sub>4</sub>@SiO<sub>2</sub>-HM-SO<sub>3</sub>H as a recyclable heterogeneous nanocatalyst for the microwave-promoted synthesis of 2,4,5-trisubstituted imidazoles under solvent free conditions. *New J. Chem.* **2015**, *39*, 9415–9421.
- (11) Sun, D.; Wang, B.; Wang, H. M.; Li, M. F.; Shi, Q.; Zheng, L.; Wang, S. F.; Liu, S. J.; Sun, R. C. Structural transformations of Hybrid Pennisetum lignin: effect of microwave-assisted hydrothermal pretreatment. *ACS Sustainable Chem. Eng.* **2019**, *7*, 3073–3082.
- (12) Egami, H.; Tamaoki, S.; Abe, M.; Ohneda, N.; Yoshimura, T.; Okamoto, T.; Odajima, H.; Mase, N.; Takeda, K.; Hamashima, Y. Scalable microwave-assisted Johnson–Claisen rearrangement with a continuous flow microwave system. *Org. Process Res. Dev.* **2018**, *22*, 1029–1033.
- (13) Ramesh, K.; Basuli, S.; Satyanarayana, G. Microwave Assisted Domino Palladium Catalysis in Water: A Diverse Synthesis of 3,3′ Disubstituted Heterocyclic Compounds. *Eur. J. Org. Chem.* **2018**, *2018*, 2171–2177.
- (14) Gawande, M. B.; Shelke, S. N.; Zboril, R.; Varma, R. S. Microwave-assisted chemistry: synthetic applications for rapid assembly of nanomaterials and organics. *Acc. Chem. Res.* **2014**, *47*, 1338–1348.
- (15) Hattori, M.; Shimamoto, D.; Ago, H.; Tsuji, M. AgPd@ Pd/TiO<sub>2</sub> nanocatalyst synthesis by microwave heating in aqueous solution for efficient hydrogen production from formic acid. *J. Mater. Chem. A* **2015**, *3*, 10666–10670.
- (16) Villemin, D.; Labiad, B. Clay catalysis: dry condensation of barbituric acid with aldehydes under microwave irradiation. *Synth. Commun.* **1990**, *20*, 3333–3337.
- (17) Qiu, G.; Dharmarathna, S.; Genuino, H.; Zhang, Y.; Huang, H.; Suib, S. L. Facile microwave-refluxing synthesis and catalytic properties of vanadium pentoxide nanomaterials. *ACS Catal.* **2011**, *1*, 1702–1709.
- (18) Praneeth, N. V.; Paria, S. Microwave-assisted one-pot synthesis of anisotropic gold nanoparticles with active high-energy facets for enhanced catalytic and metal enhanced fluorescence activities. *CrystEngComm* **2018**, *20*, 4297–4304.
- (19) Karmakar, A.; Martins, L. M.; Hazra, S.; Guedes da Silva, M. F. C.; Pombeiro, A. J. Metal–organic frameworks with pyridyl-based isophthalic acid and their catalytic applications in microwave assisted peroxidative oxidation of alcohols and Henry reaction. *Cryst. Growth Des.* **2016**, *16*, 1837–1849.
- (20) Qiu, G.; Huang, H.; Genuino, H.; Opembe, N.; Stafford, L.; Dharmarathna, S.; Suib, S. L. Microwave-assisted hydrothermal synthesis of nanosized α-Fe<sub>2</sub>O<sub>3</sub> for catalysts and adsorbents. *J. Phys. Chem. C* **2011**, *115*, 19626–19631.
- (21) Song, C.; Li, R.; Liu, F.; Feng, X.; Tan, W.; Qiu, G. Cobalt-doped todorokites prepared by refluxing at atmospheric pressure as cathode materials for Li batteries. *Electrochim. Acta* **2010**, *55*, 9157–9165.
- (22) Martín-Acosta, P.; Feresin, G.; Tapia, A.; Estévez-Braun, A. Microwave-assisted organocatalytic intramolecular Knoevenagel/hetero diels–alder reaction with O-(Arylpropynoxy)-Salicylaldehydes: synthesis of polycyclic embelin derivatives. *J. Org. Chem.* **2016**, *81*, 9738–9756.
- (23) Biswas, P.; Ghosh, J.; Maiti, S.; Bandyopadhyay, C. Microwave-induced domino-Knoevenagel-hetero Diels–Alder reaction—an easy route to di[1]benzopyrano[2,3-b:4′,3′-d] pyridine. *Tetrahedron Lett.* **2014**, *55*, 6882–6886.
- (24) Xiao, B. X.; Jiang, B.; Song, X.; Du, W.; Chen, Y. C. Phosphine-catalysed asymmetric dearomative formal [4+2] cycloadditions of 3-benzofuran vinyl ketones. *Chem. Commun.* **2019**, *55*, 3097–3100.

- (25) (a) Peña, R.; Martín, P.; Feresin, G. E.; Tapia, A.; Machín, F.; Estévez-Braun, A. Domino synthesis of embelin derivatives with antibacterial activity. *J. Nat. Prod.* **2016**, *79*, 970–977. (b) Aghazadeh, M.; Ghaemi, M.; Nozad Golikand, A.; Yousefi, T.; Jangju, E. Yttrium oxide nanoparticles prepared by heat treatment of cathodically grown yttrium hydroxide. *ISRN Ceram.* **2011**, *2011*, No. 542104.
- (26) Zhou, J. F.; Song, Y. Z.; Lv, J. S.; Gong, G. X.; Tu, S. Facile one-pot, multicomponent synthesis of pyridines under microwave irradiation. *Synth. Commun.* **2009**, *39*, 1443–1450.
- (27) Ruys, A. J.; Mai, Y. W. The nanoparticle-coating process: a potential sol-gel route to homogeneous nanocomposites. *Mater. Sci. Eng. A* **1999**, *265*, 202–207.
- (28) Zhou, C.; Liang, G.; Gu, A. Fabrication of variable frequency motors using polyester-imide-hybridized resins and hyperbranched polysiloxane coated nano-TiO<sub>2</sub>. *J. Mater. Sci.* **2015**, *50*, 7314–7325.
- (29) Hsiung, T. L.; Wang, H. P.; Wang, H. C. XANES studies of photocatalytic active species in nano TiO<sub>2</sub>-SiO<sub>2</sub>. *Radiat. Phys. Chem.* **2006**, *75*, 2042–2045.
- (30) Xu, H.; Cui, L.; Tong, N.; Gu, H. Development of high magnetization Fe<sub>3</sub>O<sub>4</sub>/polystyrene/silica nanospheres via combined miniemulsion/emulsion polymerization. *J. Am. Chem. Soc.* **2006**, *128*, 15582–15583.
- (31) Ermakova, M. A.; Ermakov, D. Y.; Cherepanova, S. V.; Plyasova, L. M. Synthesis of Ultradispersed Nickel Particles by Reduction of High-Loaded NiO-SiO<sub>2</sub> Systems Prepared by Heterophase Sol-Gel Method. *J. Phys. Chem. B* **2002**, *106*, 11922–11928.
- (32) Corrias, A.; Mountjoy, G.; Piccaluga, G.; Solinas, S. An X-ray Absorption Spectroscopy Study of the Ni K Edge in NiO-SiO<sub>2</sub> Nanocomposite Materials Prepared by the Sol-Gel Method. *J. Phys. Chem. B* **1999**, *103*, 10081–10086.
- (33) Díaz, G.; Perez-Hernandez, R.; Gomez-Cortes, A.; Benaissa, M.; Mariscal, R.; Fierro, J. L. CuO-SiO<sub>2</sub> sol-gel catalysts: characterization and catalytic properties for no reduction. *J. Catal.* **1999**, *187*, 1–14.
- (34) Armelao, L.; Barreca, D.; Bottaro, G.; Mattei, G.; Sada, C.; Tondello, E. Copper-Silica Nanocomposites Tailored by the Sol-Gel Route. *Chem. Mater.* **2005**, *17*, 1450–1456.
- (35) Chandraker, S. K.; Ghosh, M. K.; Lal, M.; Ghorai, T. K.; Shukla, R. Colorimetric sensing of Fe<sup>3+</sup> and Hg<sup>2+</sup> and photocatalytic activity of green synthesized silver nanoparticles from the leaf extract of *Sonchus arvensis* L. *New J. Chem.* **2019**, *43*, 18175–18183.
- (36) Yang, L.; Li, X.; Sun, C. Y.; Wu, H.; Wang, C. G.; Su, Z. M. A stable pillared-layer Cu (ii) metal-organic framework with magnetic properties for dye adsorption and separation. *New J. Chem.* **2017**, *41*, 3661–3666.
- (37) Pathak, S.; Ghosh, M. K.; Ghorai, T. K. Luminescence, Dye Degradation and DNA Binding Properties of a Dinuclear Nona Coordinated Y (III) Complex. *ChemistrySelect* **2018**, *3*, 13501–13506.
- (38) Umamaheswari, C.; Lakshmanan, A.; Nagarajan, N. S. Green synthesis, characterization and catalytic degradation studies of gold nanoparticles against congo red and methyl orange. *J. Photochem. Photobiol., B* **2018**, *178*, 33–39.
- (39) Mazaheri, H.; Ghaedi, M.; Azghandi, M. A.; Asfaram, A. Application of machine/statistical learning, artificial intelligence and statistical experimental design for the modeling and optimization of methylene blue and Cd (II) removal from a binary aqueous solution by natural walnut carbon. *Phys. Chem. Chem. Phys.* **2017**, *19*, 11299–11317.
- (40) Wan, J. P.; Jing, Y.; Liu, Y.; Sheng, S. Metal-free synthesis of cyano acrylates via cyanuric chloride-mediated three-component reactions involving a cascade consists of Knoevenagel condensation/cyano hydration/esterification. *RSC Adv.* **2014**, *4*, 63997–64000.
- (41) Shen, Y.; Yang, B. Synthesis of  $\alpha$ ,  $\beta$ -Unsaturated Cyanoesters Promoted by Tri-N-Butylarsine. *Synth. Commun.* **1989**, *19*, 3069–3075.
- (42) Cabello, J. A.; Campelo, J. M.; Garcia, A.; Luna, D.; Marinas, J. M. Knoevenagel condensation in the heterogeneous phase using aluminum phosphate-aluminum oxide as a new catalyst. *J. Org. Chem.* **1984**, *49*, 5195–5197.
- (43) Gholap, A. R.; Paul, V.; Srinivasan, K. V. Novel Process for the Synthesis of Class I Antiarrhythmic Agent ( $\pm$ )-Cibenzoline and Its Analogs. *Synth. Commun.* **2008**, *38*, 2967–2982.
- (44) Khan, R. H.; Mathur, R. K.; Ghosh, A. C. Tellurium (IV) tetrachloride catalysed facile Knoevenagel reaction. *Synth. Commun.* **1996**, *26*, 683–686.
- (45) Jain, K.; Chaudhuri, S.; Pal, K.; Das, K. The Knoevenagel condensation using quinine as an organocatalyst under solvent-free conditions. *New J. Chem.* **2019**, *43*, 1299–1304.
- (46) Ghosh, M. K.; Pathak, S.; Ghorai, T. K. Synthesis of Two Mononuclear Schiff Base Metal (M = Fe, Cu) Complexes: MOF Structure, Dye Degradation, H<sub>2</sub>O<sub>2</sub> Sensing, and DNA Binding Property. *ACS Omega* **2019**, *4*, 16068–16079.